Dalton Transactions

PAPER

View Article Online
View Journal | View Issue

Cite this: *Dalton Trans.*, 2014, **43**, 11286

C–H and C–O bond activation with a rhodium(I) β-diiminate complex†

Nicolle N. P. Langer,[a] Gurmeet Singh Bindra[b] and Peter H. M. Budzelaar*[b]

Complex LRh(COE) [L = (2,6-$Me_2C_6H_3NCMe)_2CH$; COE = cyclooctene] reacts with oxirane, methyloxirane and 2,2-dimethyloxirane to eventually produce LRh(COE)(CO) and alkane (methane, ethane, propane). This reaction and other aspects of the reactivity of the "LRh" fragment (hydrogenation of olefins and benzene) have been studied by density functional theory. The results indicate that for 2,2-dimethyloxirane (and probably also for methyloxirane) the reaction starts with C–H activation of a methyl group, followed by ring opening and decarbonylation. For the parent oxirane, where this path is not available, the reaction starts with C–O activation to form a 2-rhodaoxetane, which then undergoes β-elimination. More generally, easy C–H activation, which appears to be a recurring theme in this Rh chemistry, is due to a close energy matching between corresponding Rh(I) and Rh(III) complexes. For the analogous Ir complexes, preference for higher oxidation states is larger, leading to significantly higher barriers for *e.g.* hydrogenation.

Received 29th January 2014,
Accepted 26th March 2014

DOI: 10.1039/c4dt00309h

www.rsc.org/dalton

Introduction

Many complexes of the platinum group metals display activity in olefin hydrogenation and/or C–H activation, usually through mechanisms involving oxidative addition/reductive elimination steps.[1] For such reactivity to happen, two conditions must be fulfilled:

1. The reactive metal fragment must be low-valent and (highly) coordinatively unsaturated, in order to break unreactive H–H or C–H bonds.

2. The preference for a higher oxidation state must not be too strong, to avoid the complex getting "stuck" after oxidative addition.

The delicate balance between these two conditions explains why tuning of catalysts is a decidedly non-trivial art.

Over 10 years ago, we reported on the reactivity of rhodium β-diiminate complex **1a** [LRh(COE), COE = cyclooctene] in stoichiometric oxidative addition reactions,[2] as well as on its catalytic activity in olefin hydrogenation.[3] One remarkable aspect of the hydrogenation catalysis was the potential for hydrogenating tetrasubstituted olefins, which are normally among the most difficult classes of substrates. Experimental evidence pointed to a "chain walking" of the metal fragment (*via* an allyl-hydride intermediate) as part of the catalytic cycle. Interestingly, the corresponding Ir complex "LIr(COE)" (**1b**), which actually prefers an allyl-hydride structure, was found to be inactive in catalysis, forming a rather unreactive LIr(COE)$(H)_2$ "dead-end" species.

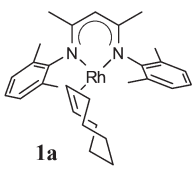

1a

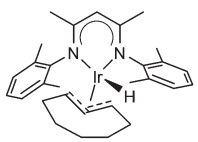

1b

We recently revisited the chemistry of complex **1a** and found that it also reacts with Si–H[4] and B–H bonds,[5] and is capable of activating even Si–Csp[3] bonds.[4] Indications were obtained that complex **1a**, or a species derived from it, is capable of (reversibly) activating C–H bonds of THF. Intrigued by this observation, we have now studied the reaction of complex **1a** with epoxides, which might be expected to undergo either C–H or C–O bond activation. In fact, we find that *both* reactions happen; interestingly, C–H activation appears to precede C–O activation. Extensive DFT studies have been carried out to elucidate the mechanism of this epoxide activation as well as details of the above-mentioned hydrogenation reactions. The results confirm earlier ideas about "chain walking" and shed light on the distinctly different reactivity patterns of analogous Rh and Ir complexes.

[a]*Department of Chemistry, Radboud University, Heyendaalseweg 135, 6525 AJ Nijmegen, The Netherlands*
[b]*Department of Chemistry, University of Manitoba, Winnipeg, MB R3 T 2N2, Canada. E-mail: Peter.Budzelaar@umanitoba.ca*

† Electronic supplementary information (ESI) available: ^1H and ^{13}C NMR spectra for reactions of **1a** with oxiranes. Total energies and thermal corrections for all species studied computationally. Energy profile for Ir analogue of Fig. 5. Atomic coordinates for all species studied. See DOI: 10.1039/c4dt00309h

Results and discussion

Activation of epoxides

LRh(COE) reacts slowly (~1 day at RT; ~1 hour at 40 °C) with methyloxirane in THF. The final product of this reaction is LRh(COE)(CO) (**2a**, Scheme 1), which was characterized by NMR. The structure of this product is presumably similar to those of the structurally characterized complexes LRh(COE)(MeCN)[3] and $L^{iPr}Rh(COE)(N_2)$.[6]

Ring opening of oxiranes mediated by Rh has been reported before,[7–9] but the emphasis has mostly been on metal-catalyzed/metal-directed nucleophilic attack rather than the present breakdown of the epoxide. Formation of **2a** plausibly involves "opening" of methyloxirane to propionaldehyde, followed by decarbonylation (Scheme 2). Indeed, reaction of **1a** with propionaldehyde rapidly produces **2a** in near-quantitative yield (by ^{1}H NMR). Decarbonylation of aldehydes at Rh has been studied both experimentally[10–13] and computationally[10] and appears to be well-understood. However, the exact mode of initial ring opening of methyloxirane is not obvious from these results. If one assumes that the first step is oxidative addition of a C–O bond to Rh, then the formation of **2a** implies a preference for attack at the substituted rather than the unsubstituted C–O bond. Attack at the unsubstituted bond would eventually produce acetone (see Scheme 2), which was not observed; moreover, treatment of **1a** with acetone did not produce any **2a**.

We then tested the reaction of **1a** with unsubstituted oxirane and with 2,2-dimethyloxirane. Reaction with oxirane was found to be even slower than with methyloxirane, and was also less clean. The main product was still **2a** but NMR spectra indicated that this was formed in only about 70% yield, and was accompanied by several unidentified by-products. In contrast, the reaction of **1a** with 2,2-dimethyloxirane was found to be much faster (~minutes at RT), while still yielding mainly **2a**. Assuming the reaction starts with C–O bond cleavage, these results would suggest a clear preference for breaking the *more highly substituted* C–O bond This is even more remarkable considering that complex **1a** has a rather bulky β-diiminate ligand, which could be expected to strongly favour attack at the less substituted bond. We also tested cyclohexene epoxide, which interestingly did not react at all with **1a**. This led us to consider the possibility that maybe C–O activation is not the first step of the reaction. In view of the reported C–H activation of THF by **1a** (or a complex derived from it),[4] initial C–H or C–C activation would also be conceivable. Based on these considerations, we came up with the five paths shown in Scheme 3 for opening of dimethyloxirane by **1a** (dimethyloxirane was chosen here because of its higher symmetry, and also because it gives the cleanest and fastest reaction). At least three of the paths could reasonably be expected to eventually produce **2a**. Distinguishing between these alternatives by experiment would be hard, so we turned to DFT methods to analyze all of them.

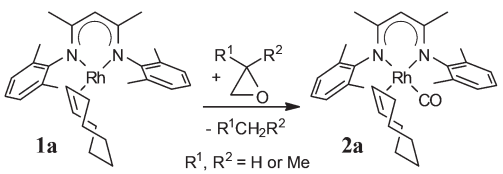

Scheme 1 Reaction of **1a** with oxiranes.

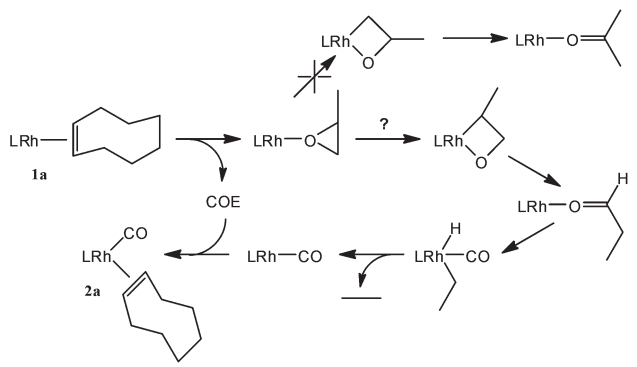

Scheme 2 Possible mechanism for formation of **2a** from **1a**.

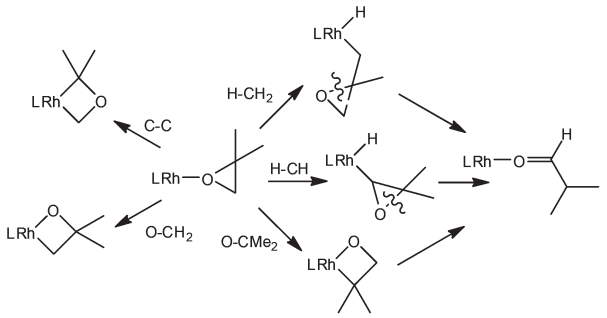

Scheme 3 Potential ring opening paths for dimethyloxirane.

DFT results for oxirane opening

Transition states were located for all paths of Scheme 3 except for a few β-eliminations, which were found to be virtually barrierless. DFT results indicate that the preferred path for ring opening of dimethyloxirane involves C–H activation of a *methyl* group. Scheme 4 shows intermediates on this path. The reaction starts with (associative) displacement of COE by the oxirane. Methyl C–H activation comes next, following by C–O cleavage. The resulting (enolate)(hydride) complex **E** undergoes insertion of the C=C bond in the Rh–H bond, followed by β-H elimination, forming (β-ketoalkyl)(hydride) species **G**. Reductive elimination now produces side-on coordinated isobutyraldehyde complex **H**, which undergoes oxidative addition of the aldehyde C–H bond, CO deinsertion, reductive elimination of alkane, and capture of COE to yield the final product (**L**).

Fig. 1 shows the geometries of important intermediates and transition states along the preferred path for ring opening (a complete set of figures for both the main path is included in the ESI†). Coordination to Rh does not affect the geometry of the oxirane much (**C**). The subsequent methyl C–H activation

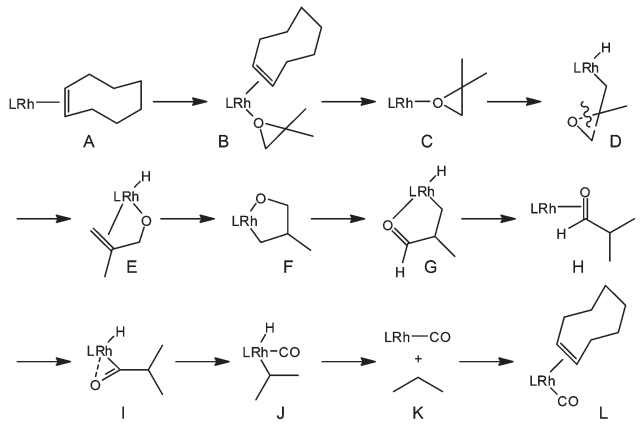

Scheme 4 Preferred path (according to DFT) for ring opening of dimethyloxirane at "LRh".

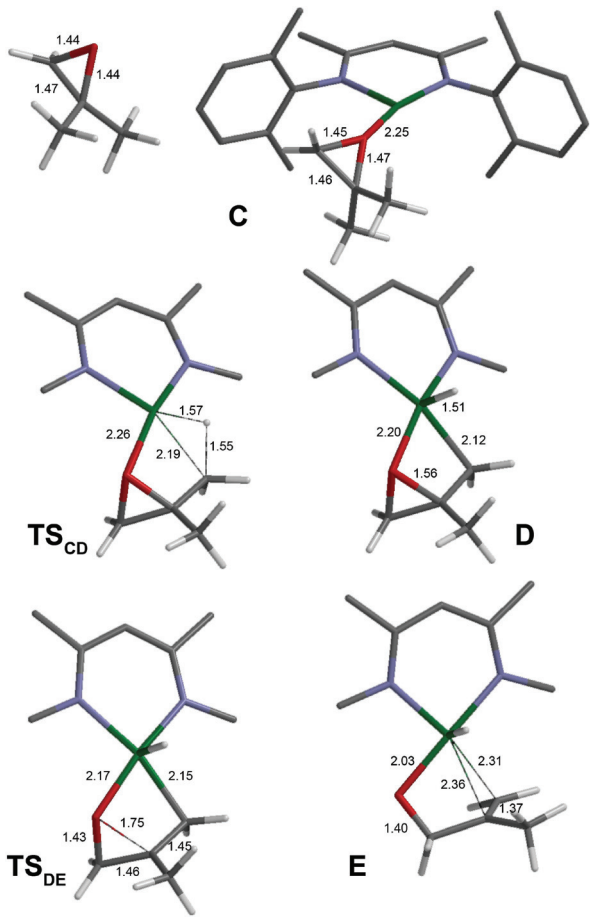

Fig. 1 Optimized structures for some intermediates and transition states along the preferred ring opening path of Scheme 3. Much of the ancillary ligand has been omitted for clarity.

occurs with retention of the O→Rh coordination, and is presumably assisted by it. The addition product (**D**) has a smaller Rh–O distance and a clearly elongated ring C–O bond (by about 0.1 Å), reflecting stronger intramolecular coordination of oxygen to Rh(III). From there, ring opening *via* $\mathbf{TS_{DE}}$ is accompanied by a further contraction of the Rh–O bond. In the path depicted in Fig. 1, the metal-bound hydride and the methyl group of the enolate in **E** end up on the same side of the enolate ring plane, resulting in easy transfer of the hydride to a ring carbon to form **F**. The initial C–H activation and ring opening can also follow a diastereomeric path, with very similar energies for each step, where the hydride and methyl groups of **E′** end up on opposite sides of the ring plane. Now, hydride transfer to form **F** is much more difficult. Instead, the lowest-energy path involves decoordination and face flipping of the double bond *via* $\mathbf{TS_{E'E}}$ to arrive at **E** and continuing from there (see the ESI† for these structures). $\mathbf{TS_{E'E}}$ is, at 10.1 kcal mol^{-1}, only 8.9 kcal mol^{-1} above **E′**, so this face flip is perfectly feasible.

Fig. 2 shows the calculated free energies for relevant species on all paths of Scheme 3 (a complete list of all energies can be found in the ESI†).

Interestingly, the results show unambiguously that C–H activation of an epoxide *methyl* C–H bond is the rate-limiting step of the preferred ring-opening path. Once this bond has been broken, C–O cleavage in the internally coordinated oxiranylmethyl complex is facile, and from there on a cascade of downhill reactions leads *via* the π-acyl complex to the final product **2a** (**L**). While there is not much precedent for this mode of oxirane ring opening, it is rather similar to the well-documented easy opening of oxiranylmethyl radicals.[14]

Initial activation of an oxirane *ring* C–H bond is nearly as easy as methyl C–H activation. However, the subsequent C–O cleavage step has a prohibitively high barrier, making this a non-productive path. C–C cleavage of the oxirane is somewhat more difficult; in addition, this step does not lead to significantly more stable products and is therefore also non-productive. Perhaps more surprisingly, direct C–O cleavage of the substituted CMe_2–O bond is not competitive either.[15] Cleavage of the unsubstituted CH_2–O bond (which is indeed easier than of the substituted bond, as expected on steric grounds) is non-productive. Thus, we conclude that *methyl* C–H activation precedes ring opening; this explains why the larger "hindrance" in dimethyloxirane does not result in a slower reaction.

For unsubstituted oxirane, the energy profile is subtly different (Fig. 3). Methyl C–H activation is obviously not poss-

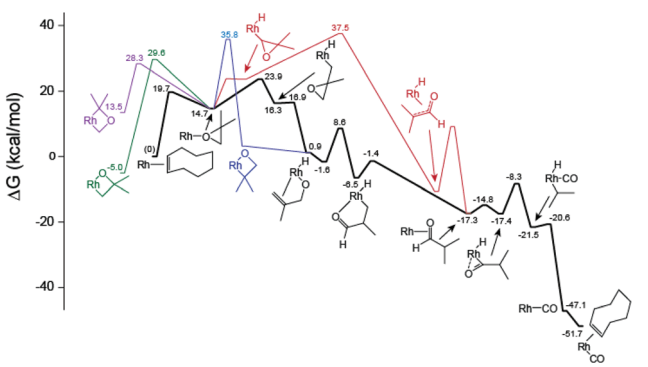

Fig. 2 Calculated free-energy profile for reaction of **1a** with 2,2-dimethyloxirane. The solid black line represents the preferred path, involving methyl C–H activation.

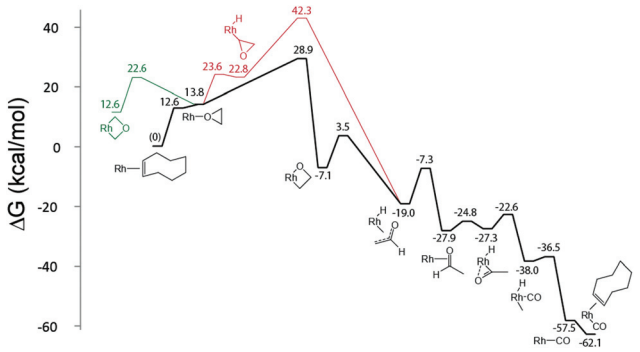

Fig. 3 Calculated free-energy profile for reaction of **1a** with oxirane. The solid black line represents the preferred path, involving ring C–O activation.

ible. Ring C–C activation has the lowest barrier but is non-productive. Ring C–H activation is feasible but the subsequent ring-opening reaction is not. However, ring C–O activation now becomes a viable mechanism; the preferred path is summarized in Scheme 5, and some relevant structures are shown in Fig. 4. The initial product of C–O activation is 2-rhodaoxetane **M′**. Only a handful of simple 2-rhodaoxetanes have been structurally characterized;[16–22] the majority derive from cyclooctadiene[16,18,21] and are stabilized by intramolecular coordination of the remaining C=C bond. The calculated structure of **M′** agrees fairly well with the X-ray structures reported for $(TPA)Rh(CH_2CH_2O)^+$ and $(MeTPA)Rh(CH_2CH_2O)^+$.[17,19] Complex **M′** easily undergoes β-elimination to give (enolate)(hydride) complex **N′**, which then undergoes reductive elimination to π-aldehyde complex **H′**, from which point the reaction proceeds as for dimethyloxirane. This calculated path roughly parallels that proposed by Milstein for reaction of oxirane with $Ir(PMe_3)_3(COE)Cl$,[23] the main difference being that in that Ir case the reaction stops at the (hydrido)(enolate) stage unless forcing conditions are employed. We tentatively ascribe the difference in reactivity in part to the higher tendency of Ir to remain at the Ir(III) oxidation state, and in part to the higher degree of unsaturation of our LRh fragment.

The calculated effective barrier for opening of oxirane (28.9 kcal mol^{-1}) is significantly higher than that for dimethyloxirane (23.7 kcal mol^{-1}), which qualitatively agrees with the higher observed rate of dimethyloxirane opening. The difference in reaction paths for the two substrates can be explained as follows:

(a) Reaction *via* O–CH_2 activation, preferred for oxirane, is non-productive for dimethyloxirane because the resulting rhodaoxetane does not have a ring β-hydrogen. Indeed, Milstein has isolated a 4,4-dimethyl-2-rhodaoxetane and found it to be quite stable.[20,22]

(b) Reaction *via* O–CMe_2 activation is blocked for dimethyloxirane because of steric hindrance.

(c) Reaction *via* methyl C–H activation provides a low-energy pathway for dimethyloxirane (and presumably monomethyloxirane) that is not available for the parent oxirane.

In this context, it should be noted that ring-lithiated oxiranes are known to rearrange to enolates.[24,25] This reaction has been studied computationally[26,27] and has a relatively high activation energy (≈ 30 kcal mol^{-1}). In view of the much lower oxophilicity of Rh compared to Li, it is perhaps not surprising that oxiranylrhodium species would not readily rearrange to enolates.

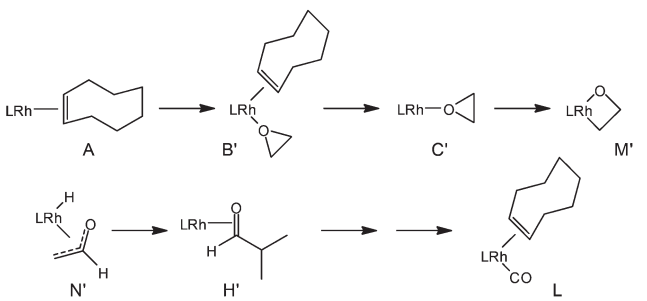

Scheme 5 Preferred path (according to DFT) for ring opening of oxirane at "LRh".

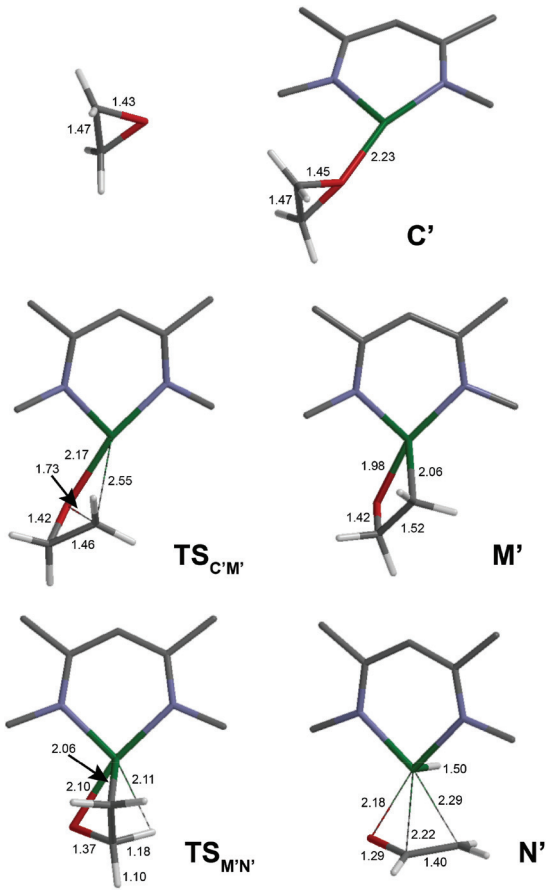

Fig. 4 Optimized structures for some intermediates and transition states along the preferred ring opening path of Scheme 5. Much of the ligand has been omitted for clarity.

Hydrogenation and C–H activation

In the absence of additional donor molecules (like N_2 or THF), LRh(COE) is fluxional, showing only two broadened ^1H resonances (ratio 6 : 8) for the COE ligand.[28] Based on calculations

for a simple model system, we proposed that in the complex the Rh "walks" around the ring *via* an allyl-hydride intermediate; the Ir analog "LIr(COE)" actually prefers such an allyl-hydride structure but is non-fluxional. In the present study we have modelled this fluxionality and subsequent hydrogenation activity, using the complete ligand in order to obtain results comparable with experiment. The results support the allyl-hydride ring walking mechanism proposed earlier; the calculated free energy of activation (14.6 kcal mol^{-1}) is compatible with the experimentally observed fluxionality,[29] and much smaller than the one calculated previously for a strongly simplified model system ($\Delta H^{\ddagger} \approx 24$ kcal mol^{-1}).[3]

Catalytic hydrogenation with "LRh" was studied computationally for COE and 2,3-dimethyl-2-butene (2-DMB) as substrates. The mechanism of COE hydrogenation is straightforward (see Fig. 5). LRh(COE) first binds a dihydrogen molecule, giving LRh(COE)(H_2), which is the resting state and has actually been observed by ^{1}H NMR.[3] This then undergoes H–H cleavage and insertion of the olefin in one of the Rh–H bonds; interestingly, our calculations indicate that there is no local minimum corresponding to a discrete dihydride complex. In any case, after insertion the resulting (alkyl)-(hydride) complex can either undergo immediate reductive elimination, or first bind a dihydrogen molecule. These alternatives appear to be close in energy; the path w*ithout* prior H_2 coordination is preferred, and has an effective barrier of 11.5 kcal mol^{-1}. The resulting cyclooctane (COA) molecule is only weakly bound to Rh and is easily lost; the remaining LRh or LRh(H_2) fragment picks up a new COE molecule to close the catalytic cycle.

From the energies of the species involved, it is clear that "ring walking" of LRh(COE) *via* the allyl-hydride mechanism is not competitive with hydrogenation. On the other hand, reversion of alkyl-hydride species back to LRh(COE)(H_2) is easy relative to the reductive elimination step, leading to the expectation that the LRh fragment could walk along the substrate backbone prior to elimination. These are important issues when considering the design of stereoselective variations of the catalysis.

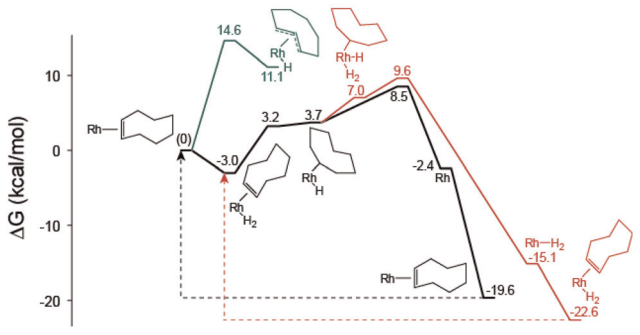

Fig. 5 Calculated free-energy profile for catalytic COE hydrogenation using **1a**. The solid black line represents the preferred path; the red line is the alternative path involving H_2 coordination prior to C–H reductive elimination. The green step corresponds to "ring walking" *via* the allyl-hydride mechanism.

Results for catalytic hydrogenation of DMB are significantly different. We have studied both the direct hydrogenation path and an indirect path involving prior isomerization of the olefin within the coordination sphere. While 2-DMB is the thermodynamically preferred isomer of the free olefin, the preferred form of the *complexed* olefin is 2,3-dimethyl-1-butene (1-DMB). The results (summarized in Fig. 6) show that the direct hydrogenation path is *more difficult* than the one involving prior isomerization (effective barrier 18.0 *vs.* 14.7 kcal mol^{-1}). Thus, it is likely that in hydrogenation of tetrasubstituted olefins with **1a** the Rh center would tend to migrate to a primary carbon, if possible, before being hydrogenated off. It should also be noted that for this more hindered olefin the resting state is not an olefin complex but LRh(H_2).

Arene hydrogenation

The reaction of LRh(COE) with hydrogen and benzene is rather subtle.[3,30] Reaction of LRh(COE) alone with H_2 in an "inert" solvent (THF or cyclohexane) initially leads to LRh(COE)(H_2), and then to a complex tentatively identified as $[LRhH]_2(\mu\text{-}H)_2$. Dissolution of LRh(COE) in benzene leads to slow (days) formation of $[LRh]_2(\mu\text{–}\eta^4\text{:}\eta^4\text{-}C_6H_6)$, which does not react with H_2. If a solution of LRh(COE) in benzene is treated with H_2 for 10 min, and the H_2 atmosphere is then removed, NMR shows that the dominant species in solution is LRh(η^4-C_6H_6), which slowly (~1 day) disproportionates to $[LRh]_2(\mu\text{–}\eta^4\text{:}\eta^4\text{-}C_6H_6)$ and C_6H_6. Finally, if a solution of LRh(COE) in benzene is kept under H_2 for one day, the main product is LRh(1,3-CHD) (CHD = cyclohexadiene). Catalytic hydrogenation of benzene was never observed, and would not be expected on thermodynamic grounds.

We have modeled this arene reactivity of LRh(COE), again using the complete ligand without simplifications. Calculated energies are summarized in Fig. 7 (formation of "LRh"/"LRh(H_2)" and COA from **1a** and H_2 has been described above and

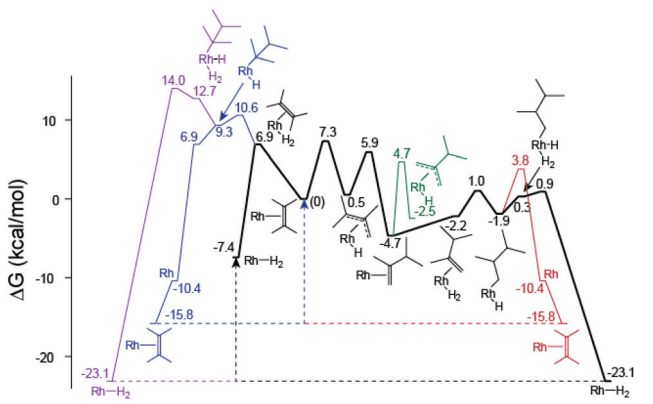

Fig. 6 Calculated free-energy profile for catalytic 2-DMB hydrogenation with "LRh". The solid black line represents the preferred path, involving isomerization and H_2 coordination prior to C–H reductive elimination. The red line corresponds to elimination without prior H_2 coordination; the blue and violet paths are without prior DMB isomerization. The green step corresponds to non-productive isomerization to a 2-^{i}Pr-allyl derivative.

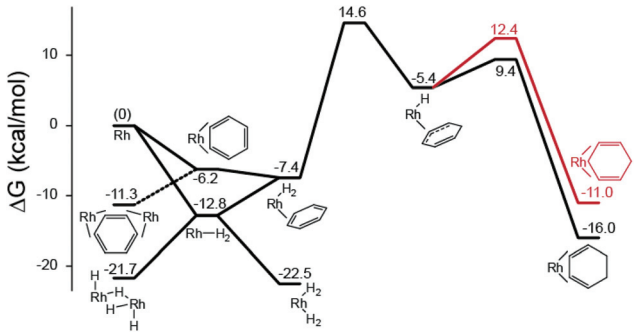

Fig. 7 Calculated free-energy profile for reaction of "LRh" with benzene and hydrogen.

is not included in the profile); geometries on the path to LRh-(1,3-CHD) are shown in Fig. 8. In the absence of added donors, formation of a dimer $[LRhH]_2(\mu\text{-}H)_2$ is indeed found to be feasible; the calculated structure shows some resemblance to silane complexes reported by Tilley.[31] $LRh(H_2)$ can also bind a second H_2 molecule, giving a bis(dihydrogen) complex (in contrast to its Ir analogue, *vide infra*). This second H_2 molecule, like the first one, is only weakly bound; based on the calculated energies one would expect easy dissociation.

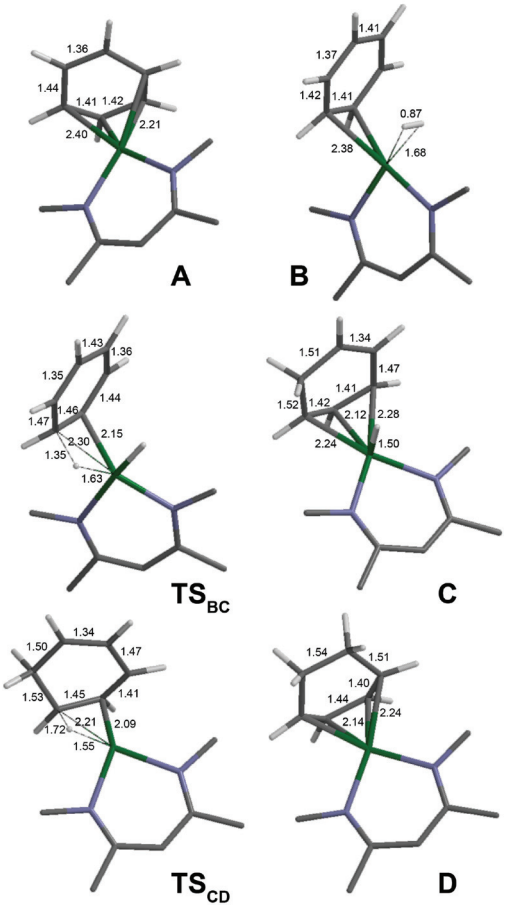

Fig. 8 Calculated structures along the path from LRh(η^4-C_6H_6) to LRh-(η^4-C_6H_8). Much of the diiminate ligand has been omitted for clarity.

Benzene binds even more weakly than H_2.[32] Calculations support the assignment (based on ^{1}H and ^{13}C NMR) of an η^4-bound structure for the adduct $LRh(C_6H_6)$ (Fig. 8, **A**), but judging from the ring bond lengths (1.36–1.44 Å) the loss of aromaticity is only partial. Coordination of H_2 to this complex, with concomitant reorganization of the C_6H_6 moiety to an η^2-bound mode (**B**), is slightly exergonic. Migration of a hydride to the benzene ring, forming LRh(η^3-C_6H_7)(H) (**C**), is the most difficult step, with a barrier of 22.0 kcal mol^{-1}. The high barrier of this step, compared to COE insertion in LRh(COE)-(H_2) (6.2 kcal mol^{-1}, *vide supra*), is likely due to the complete loss of aromaticity associated with benzene insertion. Complex **C** can then rearrange to either a 1,3-CHD or a 1,4-CHD complex; the former (**D**) is preferred on both kinetic and thermodynamic grounds. The binding of the CHD ligand in LRh(1,3-CHD) is much stronger than that of benzene in LRh-(C_6H_6) (31.8 *vs.* 6.2 kcal mol^{-1}), thus preventing ligand substitution which might have rendered the system catalytic.[33] In the absence of excess hydrogen, *i.e.* if H_2 is only used to generate "LRh" from **1a**, $[LRh]_2(\mu\text{–}\eta^4\text{:}\eta^4\text{-}C_6H_6)$ is predicted to be the preferred product, in agreement with experimental observations.

A comparison of Rh and Ir

Experimentally, LRh(COE) is a good catalyst (precursor) for olefin hydrogenation, while "LIr(COE)" on treatment with hydrogen forms unreactive $LIr(COE)H_2$.[3] To further investigate the differences in behaviour between the two metals, we calculated the Ir analogues of the Rh hydrogenation cycles discussed above. While the cycles are roughly similar, Ir shows a much stronger preference for higher oxidation states, in particular in complexes with H_2. Whereas for Rh we consistently find dihydrogen complexes, with dihydrides not even corresponding to local minima, the reverse is true for Ir, as previously reported by Chirik.[34] As an illustration, Fig. 9 compares the calculated structures of $LRh(H_2)$, $LRh(COE)(H_2)$, $LRh(H_2)_2$ with their Ir polyhydride analogues: calculated H–H bond lengths for $Rh(H_2)$ complexes are all close to 0.88 Å, whereas the H···H distances for the Ir polyhydrides vary from 1.42 to 1.64 Å. At the same time, metal–hydrogen distances are much larger for Rh (1.67–1.70 Å) than for Ir (1.56–1.58 Å).

In order to further quantify this preference, we optimized the Rh structures with H–H distances constrained to those of their Ir analogs, and *vice versa* (see Table 1). The results indicate a preference of Rh for dihydrogen complex structures of about 3–4 kcal mol^{-1}, and a similar preference of Ir for dihydride structures. Particularly noteworthy is the resistance of Rh (by about 10 kcal mol^{-1}) to form the formally pentavalent $LRhH_4$ structure.

In the context of olefin hydrogenation, the preference of Ir for higher oxidation states causes $LIr(COE)H_2$ to be a much more stable resting state than $LRh(COE)(H_2)$, and results in a rather high barrier for the path not involving extra H_2. However, the calculated effective barrier for the path *with* extra H_2 is low enough (11.6 kcal mol^{-1}) that one still would expect some hydrogenation activity *via* this route. It seems likely that the method we use underestimates the barriers of hydrogen

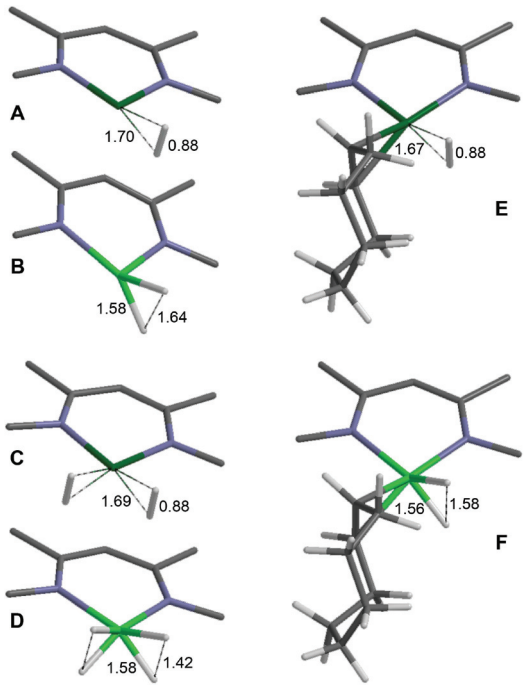

Fig. 9 Comparison of Rh dihydrogen complexes with Ir polyhydride analogues: **A** $LRh(H_2)$; **B** $LIrH_2$; **C** $LRh(H_2)_2$; **D** $LIrH_4$; **E** $LRh(COE)(H_2)$; **F** $LIr(COE)H_2$. Much of the diiminate ligand has been omitted for clarity.

Table 1 Relative energies (kcal mol^{-1}) of constrained[a] hydride and dihydrogen complexes

Constrained	E_{rel} [b]	Constrained	E_{rel} [b]
$LRhH_2$	4.20	$LIr(H_2)$	4.62
$LRh(COE)H_2$	3.37	$LIr(COE)(H_2)$	4.06
$LRhH_4$	10.58	$LIr(H_2)_2$	3.90

[a] H–H distances for Rh complexes constrained at values for Ir analogues, and *vice versa*, see Fig. 9. [b] Electronic energy relative to fully optimized structure.

transfer reactions,[35] possibly more for Ir than for Rh. The DFT results also produce virtually equal energies for the (cyclooctene) and (cyclooctenyl)(hydride) isomers of "LIr(COE)", with an interconversion barrier of only 6.6 kcal mol^{-1}. Experimentally, the equilibrium is clearly on the side of the (cyclooctenyl)(hydride) isomer, and the barrier must be significantly larger than 6.6 kcal mol^{-1} to produce static NMR spectra. We are not sure at present whether this problem is caused by the choice of functional, basis set or pseudopotential for Ir.

One reaction for which we do not yet have a satisfactory explanation is the decomposition (disproportionation) of "LIr(COE)" to $LIr(COE)H_2$ and LIr(1,4-COD). It is clear that some form of C–H activation must be involved. Also, if the reaction is carried out in THF-d_8 significant D incorporation was seen at the hydride position, indicating participation of a highly reactive, C–H activating intermediate. However, the multitude of conceivable paths, including radical reactions and ligand metallation variations, has so far precluded a definitive conclusion.

Conclusions

LRh(COE) is a relatively simple molecule giving rise to a surprising diversity of reactions, many of which involve C–H activation and several types of "chain walking". Complex reaction sequences are viable because the Rh(I) and Rh(III) oxidation states are closely balanced in this ligand environment. An example is the activation of methyloxirane and dimethyloxirane, which passes through about 10 steps before ending up in the "dead" species LRh(COE)(CO) in which finally the π-acidic CO ligand "freezes" Rh in the univalent state. In contrast, β-diiminate Ir complexes have a much larger preference for the Ir(III) [or even Ir(V)] oxidation state, leading to shorter reaction sequences, less fluxionality and less efficient catalysis.

Experimental

General

All reactions were carried out under an atmosphere of Ar in Schlenk glassware. Solvents were distilled from Na/benzophenone prior to use. Acetone was distilled and stored under N_2 on 3 Å molecular sieve. Ethylene oxide (1.2 M in THF), (±) propylene oxide and isobutylene oxide were purchased from Sigma Aldrich/TCI chemicals; the latter two were distilled under reduced pressure prior to use. LRh(COE) was prepared according to a published procedure.[3]

Reaction of LRh(COE) with methyloxirane

0.077 g of LRh(COE) was dissolved in 2.5 ml methyloxirane–diethylether (1 : 8, v : v), corresponding to a ratio Rh : methyloxirane = 1 : 30. The solution was heated for 1 hour at 40 °C. The solvent was removed *in vacuo* and the residue was dissolved in pentane. The solution was kept for one night at −30 °C. The resulting suspension was filtered and the filtrate was dried *in vacuo*, leaving LRh(COE)(CO) as a yellowish-white solid.

^{1}H NMR (300 MHz, THF-d_8, 25 °C), δ (ppm): 7.1–6.8 (m, 6H, $m + p$), 5.13 (s, 1H, β), 3.22 (m, 2H, =C*H*), 2.39, 2.21 (s, 6H each, o-CH_3), 2.11, 1.49 and 1.21 (m, 2H each, CH_2), 1.62, 1.51 (s, 3H each, N=CCH_3).

^{13}C NMR (75 MHz, THF-d_8, 25 °C), δ (ppm): 189.7 (d, J_{RhC} 73 Hz), 160.8, 159.1 (N=*C*), 159.0, 149.3 (*i*), 133.4, 131.4 (*o*), 129.2, 128.8 (*m*), 125.9, 125.5 (*p*), 98.5 (β), 79.9 (d, J_{RhC} 11 Hz, =*C*H), 32.0, 31.7, 31.2 (*C*H_2), 27.0, 22.3 (N=C*C*H_3), 19.5, 18.9 (o-*C*H_3).

IR (KBr pellet): ν_{CO} 1979 cm^{-1}.

$C_{30}H_{39}N_2ORh$ (546.53), calc (%) C 65.93, H 7.19, N 5.12; found C 64.41, H 6.97, N 5.10.

Check for acetone formation

0.0505 g of LRh(COE) was dissolved in a solution of 7.60×10^{-4} mole of methyloxirane (7.8 eq.) in THF-d_8. The solution was heated for 1 hour at 40 °C, after which an NMR spectrum was recorded. No acetone was observed. 1 equivalent of methyloxirane had been consumed to form LRh(COE)(CO), and the remaining 7 eq. was still present in the solution.

Reaction of LRh(COE) with propanal

To LRh(COE) was added an excess of a solution of propanal in diethyl ether (1 : 10). The solution was heated at 40 °C for 1 hour. The solvent was removed *in vacuo* and the residue was identified as LRh(COE)(CO) by ^{1}H and ^{13}C NMR.

Reaction of LRh(COE) with oxirane

To a purple-blue solution of LRh(COE) (0.100 g, 0.193 mmol) in 2 mL diethyl ether under an argon atmosphere was added 4.8 mL of a 1.2 M oxirane solution in THF (30 eq., 5.76 mmol). The reaction mixture turned brown immediately. After stirring for 24 hours at room temperature, the solvents were removed *in vacuo*, leaving a brownish solid which mostly consisted of LRh(COE)(CO) (^{1}H and ^{13}C NMR).

Reaction of LRh(COE) with 2,2-dimethyloxirane

Purple blue solid LRh(COE) (1.0 eq., 70 mg, 0.135 mmol) dissolved in 2 mL diethyl ether was added to anhydrous isobutylene oxide (20 eq., 0.36 mL, 4.05 mmol) under an argon atmosphere. The reaction mixture initially turned deep green and then brown. The reaction mixture was stirred at room temperature under argon for 24 hours. The solvent was evaporated *in vacuo* leaving a brownish solid which mostly consisted of LRh(COE)(CO) (^{1}H and ^{13}C NMR).

Computational details

Geometry optimizations were carried out with Turbomole[36] using the TZVP basis[37] and the b3-lyp functional[38–41] in combination with an external optimizer (PQS OPTIMIZE[42,43]). Vibrational analyses were carried out for all stationary points to confirm their nature (1 imaginary frequency for transition states, none for minima). Final energies were obtained using the TZVPP basis.[44] These were combined with thermal corrections (enthalpy and entropy, 273 K, 1 bar) from the TZVP vibrational analyses to arrive at the final free energies. To account for the reduced freedom of movement in solution, entropy contributions to the free energies were scaled to 2/3 of their gas-phase values.[45,46]

Abbreviations

COE	Cyclooctene
COA	Cyclooctane
1-DMB	2,3-Dimethyl-1-butene
2-DMB	2,3-Dimethyl-2-butene
CHD	Cyclohexadiene

Acknowledgements

We thank Mr Mark Cooper (University of Manitoba) for help with X-ray structure determinations and Prof. Frank Hawthorne for the use of their single-crystal X-ray diffractometer. This work was supported in part by NSERC, CFI, and MRIF grants (to P.H.M.B.).

Notes and references

1 D. Steinborn, *Fundamentals of Organometallic Catalysis*, Wiley-VCH, Weinheim, Germany, 2012.
2 S. T. H. Willems, P. H. M. Budzelaar, N. N. P. Moonen, R. de Gelder, J. M. M. Smits and A. W. Gal, *Chem. – Eur. J.*, 2002, **8**, 1310–1320.
3 P. H. M. Budzelaar, N. N. P. Moonen, R. de Gelder, J. M. M. Smits and A. W. Gall, *Eur. J. Inorg. Chem.*, 2000, 753–769.
4 D. Zhu, D. J. Kozera, K. D. Enns and P. H. M. Budzelaar, *Angew. Chem., Int. Ed.*, 2012, **51**, 12211–12214.
5 D. Zhu, G. S. Bindra and P. H. M. Budzelaar, to be published.
6 J. D. Masuda and D. W. Stephan, *Can. J. Chem.*, 2005, **83**, 324–327.
7 J. D. Ha, E. Y. Shin, S. K. Kang, J. H. Ahn and J. K. Choi, *Tetrahedron Lett.*, 2004, **45**, 4193–4195.
8 K. Fagnou and M. Lautens, *Org. Lett.*, 2000, **2**, 2319–2321.
9 Y. Fukumoto, N. Chatani and S. Murai, *J. Org. Chem.*, 1993, **58**, 4187–4188.
10 P. Fristrup, M. Kreis, A. Palmelund, P.-O. Norrby and R. Madsen, *J. Am. Chem. Soc.*, 2008, **130**, 5206–5215.
11 J. E. Baldwin, T. C. Barden, R. L. Pugh and W. C. Widdison, *J. Org. Chem.*, 1987, **52**, 3303–3307.
12 M. C. Baird, C. J. Nyman and G. Wilkinson, *J. Chem. Soc. A*, 1968, 348–351.
13 M. C. Baird, J. T. Mague, J. A. Osborn and G. Wilkinson, *J. Chem. Soc. A*, 1967, 1347–1360.
14 D. J. Pasto, *J. Org. Chem.*, 1996, **61**, 252–256.
15 We checked for solvent effects on the competition between C–H activation and O–CMe_2 cleavage; these were found to be minimal (see ESI† for more details).
16 C. Tejel, M. A. Ciriano, E. Sola, M. P. del Rio, G. Rios-Moreno, F. J. Lahoz and L. A. Oro, *Angew. Chem., Int. Ed.*, 2005, **44**, 3267–3271.
17 B. de Bruin, M. J. Boerakker, J. A. W. Verhagen, R. de Gelder, J. M. M. Smits and A. W. Gal, *Chem. – Eur. J.*, 2000, **6**, 298–312.
18 B. de Bruin, J. A. Brands, J. Donners, M. P. J. Donners, R. de Gelder, J. M. M. Smits, A. W. Gal and A. L. Spek, *Chem. – Eur. J.*, 1999, **5**, 2921–2936.
19 B. deBruin, M. J. Boerakker, J. Donners, B. E. C. Christiaans, P. P. J. Schlebos, R. deGelder, J. M. M. Smits, A. L. Spek and A. W. Gal, *Angew. Chem., Int. Ed. Engl.*, 1997, **36**, 2064–2067.

20 M. J. Calhorda, A. M. Galvao, C. Unaleroglu, A. A. Zlota, F. Frolow and D. Milstein, *Organometallics*, 1993, **12**, 3316–3325.
21 V. W. Day, W. G. Klemperer, S. P. Lockledge and D. J. Main, *J. Am. Chem. Soc.*, 1990, **112**, 2031–2033.
22 A. A. Zlota, F. Frolow and D. Milstein, *J. Am. Chem. Soc.*, 1990, **112**, 6411–6413.
23 D. Milstein and J. C. Calabrese, *J. Am. Chem. Soc.*, 1982, **104**, 3773–3774.
24 D. M. Hodgson, P. G. Humphreys and S. R. Hughes, *Pure Appl. Chem.*, 2007, **79**, 269–279.
25 V. Capriati, S. Florio, F. M. Perna, A. Salomone, A. Abbotto, M. Amedjkouh and S. O. N. Lill, *Chem. – Eur. J.*, 2009, **15**, 7958–7979.
26 B. R. Ramachandran, S. Waithe and L. M. Pratt, *J. Org. Chem.*, 2013, **78**, 10776–10783.
27 A. Bouyacoub, R. Hadjadj-Aoul and F. Volatron, *Eur. J. Org. Chem.*, 2008, 4466–4474.
28 P. H. M. Budzelaar, R. de Gelder and A. W. Gal, *Organometallics*, 1998, **17**, 4121–4123.
29 Precise determination of activation parameters from the NMR spectra is not possible because the slow-exchange spectrum is much too complicated to allow full simulation of dynamic effects. However, an estimated "coalescence temperature" of ~−10 °C and a "Δδ" of ~2 ppm produce an estimated free energy of activation of ~11.5 kcal mol^{-1}.
30 P. H. M. Budzelaar, N. N. P. Moonen, R. de Gelder, J. M. M. Smits and A. W. Gal, *Chem. – Eur. J.*, 2000, **6**, 2740–2747.
31 J. L. McBee and T. D. Tilley, *Organometallics*, 2009, **28**, 5072–5081.
32 The level of theory employed probably underestimates the benzene binding energy. According to ^{1}H NMR, benzene does not exchange rapidly at room temperature.
33 Catalysis producing CHD would not have been expected anyway since the reaction $C_6H_6 + H_2 \rightarrow C_6H_8$ is endergonic. Complete hydrogenation to cyclohexane would be exergonic but was never observed.
34 W. H. Bernskoetter, E. Lobkovsky and P. J. Chirik, *Chem. Commun.*, 2004, 764–765.
35 G. Talarico, A. N. J. Blok, T. K. Woo and L. Cavallo, *Organometallics*, 2002, **21**, 4939–4949.
36 *TURBOMOLE V6.3*, a development of University of Karlsruhe and Forschungszentrum Karlsruhe GmbH, 1989–2007, TURBOMOLE GmbH, since 2007, Karlsruhe, 2011.
37 A. Schäfer, C. Huber and R. Ahlrichs, *J. Chem. Phys.*, 1994, **100**, 5829–5835.
38 C. T. Lee, W. T. Yang and R. G. Parr, *Phys. Rev. B: Condens. Matter*, 1988, **37**, 785–789.
39 A. D. Becke, *J. Chem. Phys.*, 1993, **98**, 5648–5652.
40 A. D. Becke, *J. Chem. Phys.*, 1993, **98**, 1372–1377.
41 The Turbomole functional "b3-lyp" is similar (but not identical) to the Gaussian "B3LYP" functional.
42 PQS and J. Baker, *Parallel Quantum Solutions*, Fayetteville, AR, 2001.
43 J. Baker, *J. Comput. Chem.*, 1986, **7**, 385–395.
44 F. Weigend, F. Furche and R. Ahlrichs, *J. Chem. Phys.*, 2003, **119**, 12753–12762.
45 R. Raucoules, T. de Bruin, P. Raybaud and C. Adamo, *Organometallics*, 2009, **28**, 5358–5367.
46 S. Tobisch and T. Ziegler, *J. Am. Chem. Soc.*, 2004, **126**, 9059–9071.